Torque Spectroscopy of DNA: Base-Pair Stability, Boundary Effects, Backbending, and Breathing Dynamics

Florian C. Oberstrass,[1] Louis E. Fernandes,[2] Paul Lebel,[3] and Zev Bryant[1,4,*]

[1]*Department of Bioengineering, Stanford University, Stanford, California 94305, USA*
[2]*Program in Biophysics, Stanford University, Stanford, California 94305, USA*
[3]*Department of Applied Physics, Stanford University, Stanford, California 94305, USA*
[4]*Department of Structural Biology, Stanford University Medical Center, Stanford, California 94305, USA*

Changes in global DNA linking number can be accommodated by localized changes in helical structure. We have used single-molecule torque measurements to investigate sequence-specific strand separation and Z-DNA formation. By controlling the boundary conditions at the edges of sequences of interest, we have confirmed theoretical predictions of distinctive boundary-dependent backbending patterns in torque-twist relationships. Abrupt torque jumps are associated with the formation and collapse of DNA bubbles, permitting direct observations of DNA breathing dynamics.

Force spectroscopy of biomolecules has stimulated general insights into the thermodynamics of small systems [1], including experimental tests of results from nonequilibrium statistical mechanics [2–4], and theoretical investigations of ensemble inequivalence [5–7]. To enable analogous contributions from torque spectroscopy, we have recently introduced a high-resolution approach [8] for measuring the torsional response of short 20–100 base pair (bp) sequences of interest (SOI), building on previous torque measurements that revealed sequence-averaged properties of long (2–15 kbp) duplexes [8–10]. Local sequence-specific responses to supercoiling are relevant to the regulation of biological processes such as transcription [11] and replication [12,13]. The associated torque signatures [8] illustrate general features of finite systems with constrained extensive properties, analogous to an Ising model at fixed magnetization (IMFM) [14].

In our initial study [8], we measured torque signatures of right-handed to left-handed transitions in $d(p\mathrm{G}p\mathrm{C})_n$ sequences and disruption of strand-strand interactions in mismatched duplexes. For all the sequences we analyzed, we found good agreement with a 1D theoretical treatment of cooperative transitions, in which each base pair can adopt two available helical states, and junctions are disfavored by a domain wall penalty J. However, we performed only limited tests of theoretical predictions; we were unable to study the biologically important phenomenon of localized AT-rich strand separation [12], and we did not investigate reversible dynamics.

For the current study, we designed a new set of molecular constructs and characterized their responses using the "static RBT" [8,15] method. We previously described two distinct methods for measuring torque-twist relationships [8]. Both methods are based on rotor bead tracking (RBT), in which a DNA molecule is stretched using a micron-scale magnetic bead as a force handle, and rotation is monitored using a submicron nonmagnetic bead attached to the side of the DNA. In "dynamic RBT", torque is measured via the angular velocity of a calibrated viscous load. In static RBT, a reference DNA segment is used as a calibrated torsional spring [Fig. 1(a)]. We have chosen static RBT here because it allows the use of smaller rotational probes, improving torque resolution [8,15].

Figure 1(b) shows the response of a 50 bp long GC-repeat (Z50), a representative SOI that we previously investigated extensively using dynamic RBT [8]. For small twisting deformations, the molecule shows linear torsional elasticity characteristic of standard right-handed B-form DNA. At high levels of underwinding, the torsional response switches to a second linear region; the negative shift along the twist axis is consistent with a transformation to left-handed Z-DNA. The intervening region shows a characteristic abrupt torque jump associated with formation of a Z-DNA domain, and a B-Z coexistence region in which the torque is approximately constant. As seen in our dynamic RBT experiments [8], the torque-twist relationship is well described by an Ising-type model (see Supplemental Material [16]) whose parameters include the changes in twist $\Delta\theta_0$, free energy ΔG_0, and torsional compliance Δc_t associated with the state transition for a single base pair. The best-fit values for these parameters and for the domain wall penalty J are in good agreement with our dynamic RBT results (Fig. S1 and Table S1 [16]).

We analyzed boundary effects in order to design rigorous challenges of our previous model. In the Z50 construct described above, the SOI is embedded in a continuous sequence with flanking regions of low Z propensity. Our corresponding model calculations make use of "fixed boundary conditions": we assume that the bases adjacent to the edges of the SOI remain in B-form, and a domain wall penalty is assessed if a base pair at the edge of the SOI adopts the Z-DNA state. In an alternative scenario, under
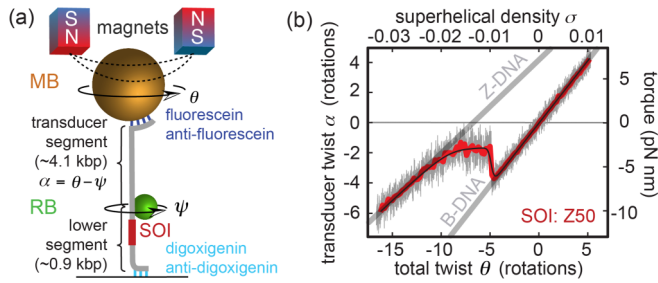
FIG. 1 (color online). Static RBT assay for high-resolution torque spectroscopy. (a) A DNA tether is attached between the cover glass surface and a magnetic bead (MB), with torsional constraints at both ends. A rotor bead (RB) is attached site specifically to the side of the DNA molecule. The total twist θ is controlled by the angular position of the magnets. Transducer twist α is given by $\alpha = \theta - \psi$, where ψ is the angular position of the RB. The torque τ acting on the DNA can be calculated as $\tau = \kappa_{TD}\alpha$, where κ_{TD} is the torsional spring constant of the calibrated transducer segment. A sequence of interest (SOI, red) is inserted in the lower DNA segment. (b) Torque is plotted as a function of imposed twist for a DNA containing a 50 bp long $d(pGpC)$-repeat SOI (Z50). Data are shown for winding in the $(+)$ direction only (see Fig. S1 [16] for overlaid unwinding and rewinding curves). Raw 250 Hz data (gray) were averaged in 0.2 rotation bins (red) and fit to a model for cooperative structural transitions in polymers [8] with fixed boundary conditions (black line, Eq. S7 [16]). The curve shows a transition between two linear elastic regions corresponding to B-DNA and Z-DNA (gray lines). Superhelical density $\sigma = \Delta Lk / Lk_0$, where Lk_0 is the linking number of the relaxed DNA ($Lk_0 = N_{total}/10.4$, where N_{total} is the length of the full DNA construct in base pairs) and $\Delta Lk = \theta$ for our experimental geometry.

"free boundary conditions", the SOI is considered to be uncoupled from its surroundings, and there is never a domain wall penalty assessed at either edge of the SOI. For a given parameter set, these two conditions can predict very different responses (Fig. 2).

In our treatment of Z50 and in related physical models, domain wall penalties lead to "overshoot" features in plots of mean torque as a function of imposed twist. Under fixed boundary conditions, there is an abrupt torque jump at the beginning of the transition as an initial domain is formed (Figs. 1(b) and 2(a), and Fig. S2 [16]). This domain then grows, and domain walls persist in the final all-Z configuration. In contrast, under free boundary conditions (Figs. 2(b) and 2(c), and Fig. S2 [16]) there are no domain-wall penalties in the final configuration, and as a result there are two abrupt transitions: a torque overshoot as an initial nucleus is formed, followed later by an "undershoot" as the molecule abruptly transitions from partially converted to fully converted, ridding itself of domain walls. We previously presented the partition functions for both fixed and free boundary conditions [8]. We also described an experimental realization proposed to approximate free boundary conditions, in which atomic spacers (Table S3
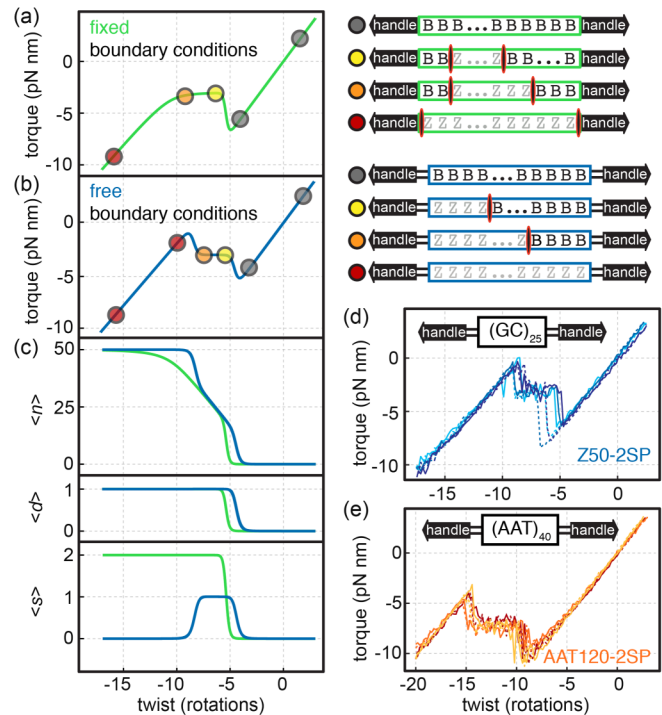

FIG. 2 (color online). Torque-twist signatures of free boundary conditions and the behavior of a 100% AT sequence. (a) Average values for torque and other variables were calculated as a function of imposed twist for a transition with fixed boundary conditions using parameters measured for Z50 (Table S1 [16]). Schematic depictions show representative microstates for portions of the torque-twist curves marked with colored dots. The SOI is outlined as a green rectangle. Domain walls are shown as red and black ovals. (b) Calculations and illustrations for the transition of Z50 under free boundary conditions (blue), shown as in (a). (c) calculations of number of nucleotides, n in the high-energy state, number of domains, d, in the high-energy state, number of domain walls, s, for Z50 as a function of imposed twist under fixed (green) and free (blue) boundary conditions. (d)–(e) Measured torque-twist plots. For each construct, three independent experiments are shown; dashed and solid lines indicate $(-)$ and $(+)$ winding directions, respectively. (d) Z50 SOI flanked by atomic spacers (Z50-2SP). (e) 120 bp AAT-repeat SOI flanked by atomic spacers (AAT120-2SP).

[16]) placed at the edges of the SOI isolate the sequence from the surrounding DNA, while preserving a torsional constraint [8]. However, we tested these atomic spacers only with short sequences that show two-state behavior, and did not discuss or investigate the overshoot-undershoot behavior described above.

AAT- and GC repeats show torque undershoots predicted for free boundary conditions.—We measured torque as a function of the imposed twist for two new constructs in which a long SOI is flanked by atomic spacers. In Z50-2SP, the SOI is the 50 bp Z-forming GC-repeat studied earlier. In AAT120-2SP, we used a 120 bp AAT-repeat that we predicted would readily undergo strand separation. Both
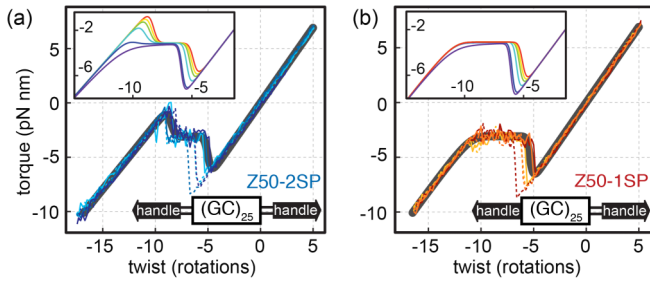
FIG. 3 (color online). The effect of boundary conditions on transitions in GC-repeats. (a) Torque-twist plots for Z50-2SP acquired during unwinding (dashed blue lines) and rewinding (solid blue lines) together with a fit (gray) to a generalized model (equations in the Supplemental Material [16]) which includes a variable boundary penalty J' for domain walls at the edges of the SOI. Inset, calculated plots for $J' = 0, 0.5, 1, 2, 4$ and $J' = J = 5.6$ kcal/mol are in red, yellow, green, light blue, dark blue, and violet, respectively. All other parameters have been kept constant (Table S1, Z50-2SP, Ref. [16]). The generalized model reduces to free boundary conditions for $J' = 0$ and to fixed boundary conditions for $J' = J$. (b) Torque-twist plots for Z50-1SP, which contains an atomic spacer on only one side of the SOI, are shown together with a fit to a one-sided model. Inset shows the effect of varying J' on the one-sided model, with color-coding as in (a) ranging from $J' = 0$ to $J' = J = 6.3$ kcal/mol (all other parameters taken from Table S1, Z50-1SP, Ref. [16]).

constructs show the predicted overshoot and undershoot features surrounding the torque plateau [Figs. 2(d) and 2(e)]. Torque-twist plots collected for AAT120-2SP show no perceptible hysteresis under our conditions, and we have used averaged unwinding and rewinding curves for subsequent equilibrium analysis. For Z50-2SP, we observe some hysteresis, and have used rewinding curves as an approximation for equilibrium curves in subsequent analysis, as before [8].

To allow quantitative fits to torque-twist curves containing atomic spacers, we introduce a generalized model that includes "free" and "fixed" boundary conditions as

special cases (Eq. S13 [16]). We account for variable coupling with the surrounding DNA by including a parameter J' that represents a penalty assessed for a domain wall that occurs at the edge of the SOI. This model reduces to fixed boundary conditions for $J' = J$ and to free boundary conditions for $J' = 0$ [Fig. 3(a), inset]. By fitting the response of Z50-2SP using this model, we measure $\Delta G = 0.5$ kcal/(molbp), $J = 5.6$ kcal/mol, and $\Delta\theta_0 = -1.1$ rad/bp, agreeing well with fits to spacer-free Z50 (Fig. 3(a) and Table S1 [16]). As expected, the edge-specific domain wall penalty was found to be low, $J' = 1$ kcal/mol, supporting our proposal that atomic spacers create a close approximation to free boundary conditions. To further test this result and challenge our model, we constructed DNA tethers with a spacer on only one side of the SOI [Z50-1SP, Fig. 3(b)], and fit to a one-sided generalized model (Eq. S14 [16]). Measurements closely match the predicted shape of the torque-twist relationship, and the parameters extracted from Z50-1SP data are in good agreement with Z50-2SP measurements, including $J' \approx 1$ kcal/mol (Fig. 3(b) and Table S1 [16]).

AAT-repeats undergo strand-separation when underwound.—We used the generalized model to extract thermodynamic and structural parameters from the AAT120-2SP data (Fig. 4(b), Tables S1 and S2 [16]). For this equilibrium torque-twist curve, the best fit $J' = 0.5$ kcal/mol reinforces our conclusion that atomic spacers efficiently abrogate coupling. The fit values $\Delta\theta_0 = -0.6$ rad/bp and $\Delta G = 0.6$ kcal/(mol bp) are consistent with expectations for strand separation, based on (i) assuming complete loss of B-form helicity (B-form twist = 0.60 rad/bp) and (ii) predicting the thermodynamic stability of AAT-repeats from the unified view of polymer nearest-neighbor thermodynamics for strand separation [17] or more recent force spectroscopy analysis [18]. The best fit $J = 7$ kcal/mol provides a direct measurement of the domain wall penalty underlying the cooperativity of DNA melting, and is slightly larger than previous estimates based
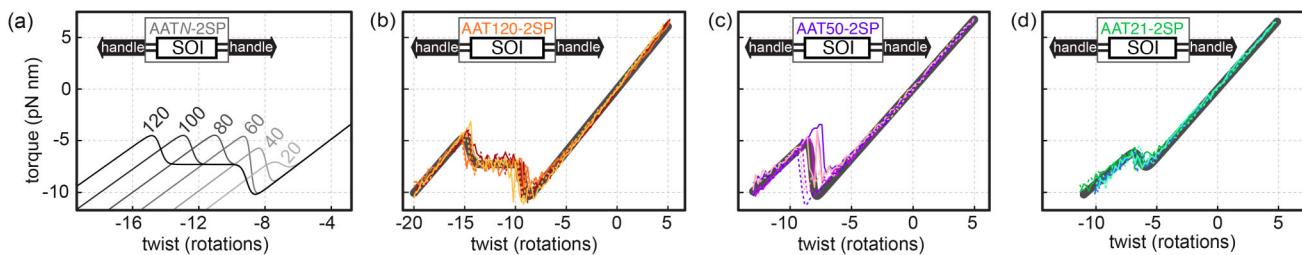

FIG. 4 (color online). The effect of SOI length on transitions in AAT-repeats. (a) Series of calculated torque-twist plots using the model with free boundary conditions and SOI lengths ranging from $N = 20$ to $N = 120$ bp (all other parameters fixed based on AAT120-2SP, Table S1 [16]). (b) Torque-twist plots of three independent AAT120-2SP unwinding (dashed thin lines) and rewinding (solid thin lines) experiments are overlaid with model fits (bold line). (c) Torque-twist plots of three independent AAT50-2SP unwinding (dashed) and rewinding (solid) experiments together with a fit in which ΔG_0, J, and J' are fixed based on AAT120-2SP (Table S1 [16]). (d) Torque-twist plots of three independent AAT21-2SP unwinding (dashed) and rewinding (solid) experiments. The model displayed (gray bold line) uses the parameters shown in Supplemental Material Table S1 (AAT21-2SP) [16].
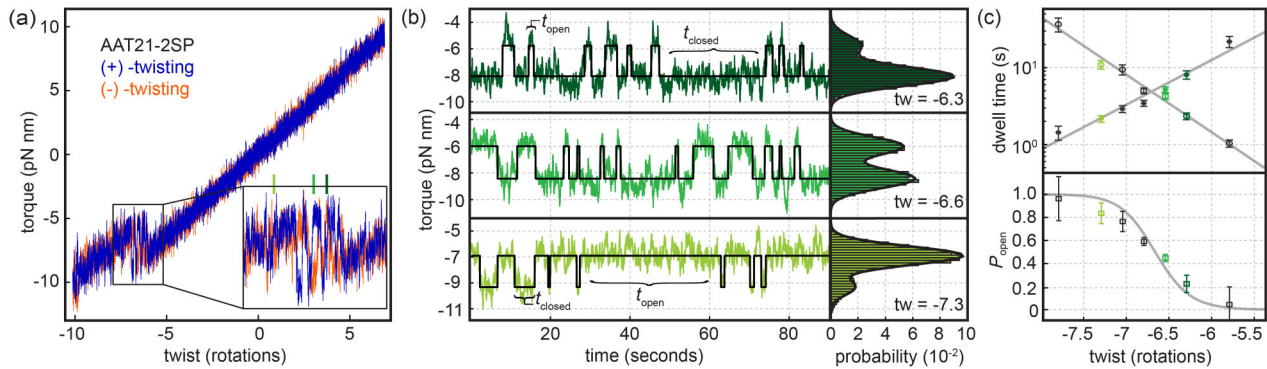
FIG. 5 (color online).   ''Breathing'' dynamics of 21 bp AAT-repeats. (a) Torque response of the AAT21-2SP SOI during linear twist ramps (10 deg/s) in the (−)-twisting and (+)-twisting directions. The inset contains an expanded view of the transition region, showing reversible hopping. Green lines are used to indicate twist values used for fixed-twist dynamic experiments shown in subsequent panels. (b) Raw data are overlaid with two-state idealizations (black line) used to measure t_{open} and t_{closed} as shown. Torque histograms at the right of each panel were generated from the entire 800 s of data collected at each twist condition, and are overlaid with double Gaussian fits. (c) Semi-log plot of mean dwell times $\langle t_{open} \rangle$ and $\langle t_{closed} \rangle$ as a function of total imposed twist (top panel). Probabilities of being in the open state at fixed twists are fit using a two-state model (Eq. S2 [16]). The fit gives a total ΔG_0 of 12 kcal/mol; κ_0, $\Delta \theta_0$, and Δc_t were fixed based on linear fits to the torque-twist curve for this SOI (AAT21-2SP) as described in Table S1 [16].

on thermal melting [19] and bulk topoisomer analysis [20,21]. The AAT120-2SP measurements provide a model system for superhelically driven destabilization in AT-rich sequences, and are also directly relevant to the behavior of AAT triplet repeats *in vivo*; previous bulk measurements have shown that AAT repeats undergo helix opening in supercoiled plasmids [22]. Spacer-free AAT120 constructs more closely represent AT-rich sequences in their biological context; torque-twist plots for these constructs also show clear transitions, which display the fingerprint of fixed boundary conditions as expected (Fig. S5 [16]).

Short AAT repeats show two-state behavior.—As discussed, SOIs with large Ns under free boundary conditions show two abrupt torque jumps flanking a plateau. Lowering N is expected to shorten the transition plateau until the torque jumps merge into a single rip, approximating a two-state transition (Fig. 4(a), Figs. S3 and S4 [16]). Measurements on AAT-repeats show the expected behavior. We tested AAT-repeats with a total of $N = 50$ (AAT50-2SP) and $N = 21$ (AAT21-2SP) base pairs [Figs. 4(c) and 4(d)]. The measured torque response of AAT50-2SP and AAT21-2SP match our predictions and are consistent with parameters measured for AAT120-2SP (Fig. 4 and Table S1 [16]).

Short-lived dynamic duplex opening (DNA ''breathing'') has been studied because of its relevance to kinetic mechanisms of biological processes [23,24]. AAT21-2SP exhibits two-state behavior and shows reversible transitions under our conditions (Figs. 4(d) and 5(a), and Fig. S4 [16]). We observe reversible hopping between the two states (strand-separated or ''open'' and B-form or ''closed'') during twist ramps [Fig. 5(a)]. Long observations at fixed twist show many reversible transitions and allow the measurement of state lifetimes for open and closed conformations. An increase in negative twist

shifts the equilibrium from the closed to the open state (Figs. 5(b) and 5(c) and Fig. S6 [16]).

Backbending features in isotherms are a general property of cooperative transitions in small systems under external constraints.—These features have been analyzed theoretically in the IMFM [14], which has been applied to diverse phenomena [25] including transitions of adatom clusters on a surface [26]. Torque overshoots in the fixed linking number ensemble have also been studied in the case of plectonemic buckling: abrupt torque jumps at this transition have been inferred to accompany abrupt extension jumps [27,28]; they have been predicted from theory and simulation [28,29], measured with the help of lock-in detection [30], and directly observed using dynamic RBT and electromagnetic torque tweezers [8,31]. At the buckling transition, the free energy associated with forming a plectonemic end loop [29] plays a role analogous to the domain wall penalty J, adding an energetic cost to the initial formation of a plectonemic domain.

Local strand separation in superhelical DNA is critical for biological functions [23,24,32]. In this study, we have observed duplex opening dynamics and have also measured structural, mechanical, and thermodynamic parameters for strand separation alongside measurements of the competing [33] B-Z transition (Table S2 and accompanying note [16]). After parameterization with simple SOIs, our theoretical treatment of cooperative structural transitions can be extended to predict the torque responses of complex biological sequences.

*To whom all correspondence should be addressed.
zevry@stanford.edu

[1] A. Mossa, J.M. Huguet, and F. Ritort, Physica (Amsterdam) **42E,** 666 (2010).

[2] J. Liphardt et al., Science **296,** 1832 (2002).

[3] D. Collin, F. Ritort, C. Jarzynski, S.B. Smith, I. Tinoco, and C. Bustamante, Nature (London) **437,** 231 (2005).

[4] A. Alemany, A. Mossa, I. Junier, and F. Ritort, Nat. Phys. **8,** 688 (2012).

[5] D. Keller, D. Swigon, and C. Bustamante, Biophys. J. **84,** 733 (2003).

[6] S. Sinha and J. Samuel, Phys. Rev. E **71,** 021104 (2005).

[7] M. Suzen, M. Sega, and C. Holm, Phys. Rev. E **79,** 051118 (2009).

[8] F.C. Oberstrass, L.E. Fernandes, and Z. Bryant, Proc. Natl. Acad. Sci. U.S.A. **109,** 6106 (2012).

[9] Z. Bryant, M.D. Stone, J. Gore, S.B. Smith, N.R. Cozzarelli, and C. Bustamante, Nature (London) **424,** 338 (2003).

[10] M.Y. Sheinin, S. Forth, J.F. Marko, and M.D. Wang, Phys. Rev. Lett. **107,** 108102 (2011).

[11] V. Vijayan, R. Zuzow, and E.K. O'Shea, Proc. Natl. Acad. Sci. U.S.A. **106,** 22 564 (2009).

[12] D. Kowalski, D.A. Natale, and M.J. Eddy, Proc. Natl. Acad. Sci. U.S.A. **85,** 9464 (1988).

[13] U. von Freiesleben and K.V. Rasmussen, Res. Microbiol. **143,** 655 (1992).

[14] F. Gulminelli, J.M. Carmona, Ph. Chomaz, J. Richert, S. Jiménez, and V. Regnard, Phys. Rev. E **68,** 026119 (2003).

[15] Z. Bryant, F.C. Oberstrass, and A. Basu, Curr. Opin. Struct. Biol. **22,** 304 (2012).

[16] See Supplemental Material at http://link.aps.org/supplemental/10.1103/PhysRevLett.110.178103 for methods, equations, additional figures, and tables.

[17] J. SantaLucia, Jr., Proc. Natl. Acad. Sci. U.S.A. **95,** 1460 (1998).

[18] J.M. Huguet, C.V. Bizarro, N. Forns, S.B. Smith, C. Bustamante, and F. Ritort, Proc. Natl. Acad. Sci. U.S.A. **107,** 15 431 (2010).

[19] B.R. Amirikyan, A.V. Vologodskii, and L. Lyubchenko Yu, Nucleic Acids Res. **9,** 5469 (1981).

[20] C.J. Benham, J. Mol. Biol. **225,** 835 (1992).

[21] W.R. Bauer and C.J. Benham, J. Mol. Biol. **234,** 1184 (1993).

[22] K. Ohshima et al., J. Biol. Chem. **271,** 16 784 (1996).

[23] A. Krueger, E. Protozanova, and M.D. Frank-Kamenetskii, Biophys. J. **90,** 3091 (2006).

[24] T. Ambjornsson, S.K. Banik, O. Krichevsky, and R. Metzler, Biophys. J. **92,** 2674 (2007).

[25] M. Pleimling and A. Huller, J. Stat. Phys. **104,** 971 (2001).

[26] W. Selke and T. Müller, Eur. Phys. J. B **10,** 549 (1999).

[27] S. Forth, C. Deufel, M. Sheinin, B. Daniels, J.P. Sethna, and M.D. Wang, Phys. Rev. Lett. **100,** 148301 (2008).

[28] H. Brutzer, N. Luzzietti, D. Klaue, and R. Seidel, Biophys. J. **98,** 1267 (2010).

[29] J.F. Marko and S. Neukirch, Phys. Rev. E **85,** 011908 (2012).

[30] B.C. Daniels, S. Forth, M. Sheinin, M.D. Wang, and J.P. Sethna, Phys. Rev. E **80,** 040901(R) (2009).

[31] X.J. Janssen, J. Lipfert, T. Jager, R. Daudey, J. Beekman, and N.H. Dekker, Nano Lett. **12,** 3634 (2012).

[32] B.S. Alexandrov, V. Gelev, S.W. Yoo, L.B. Alexandrov, Y. Fukuyo, A.R. Bishop, K.O. Rasmussen, and A. Usheva, Nucleic Acids Res. **38,** 1790 (2010).

[33] J.V. Ditlevson, S. Tornaletti, B.P. Belotserkovskii, V. Teijeiro, G. Wang, K.M. Vasquez, and P.C. Hanawalt, Nucleic Acids Res. **36,** 3163 (2008).